JOURNAL OF STRUCTURAL BIOLOGY 112, 32–40 (1994)

Analysis of Immunolabeled Cells by Atomic Force Microscopy, Optical Microscopy, and Flow Cytometry

C. NEAGU,* K. O. VAN DER WERF, C. A. J. PUTMAN, Y. M. KRAAN, B. G. DE GROOTH, N. F. VAN HULST, AND J. GREVE

*MESA-Research Institute, University of Twente, P.O. Box 217, 7500 AE Enschede, The Netherlands; and Department of Applied Physics, University of Twente, P.O. Box 217, 7500 AE Enschede, The Netherlands

Received November 15, 1993, and in revised form February 4, 1994

In this study we investigated the applicability of the (silver-enhanced) immunogold labeling method for atomic force microscopy. Human lymphocytes were labeled with anti-CD3 conjugated to fluorescein isothiocyanate and a secondary antibody (goat anti-mouse) linked with 1- or 30-nm colloidal gold particles. Silver enhancement was applied on these labeled cells to increase the size of the labels. In a setup combining an inverted optical microscope and a stand-alone atomic force microscope, a direct correlation was made between the force and the fluorescent images. Additionally, we performed flow cytometric analysis. From the results we conclude that immunogold labeling using small labels (1 nm) in combination with silver enhancement (30 min) proves to be a reliable method for high-resolution cell surface antigen detection in atomic force microscopy. © 1994 Academic Press, Inc.

INTRODUCTION

A prerequisite for a microscopic technique to be widely applicable to biological objects is that there are means to identify specific structures in the image. Unless the lateral resolution is sufficient for a direct structural identification of substructures, labeling techniques have to be used. In optical microscopy, labels include absorption and fluorescent and phosphorescent dyes. Sometimes the label itself has the required specificity (e.g., DNA stains like propidium iodide or mitramicin), but in general the specificity has to be added by linking the label to a molecule that binds specifically to the structure of interest. An important class of molecules that can be used to add specificity to a label are the (monoclonal) antibodies that can be raised against almost all biological structures. Antibodies conjugated with colloidal gold spheres (immunogold labels) are used in light microscopy (LM; Hoefsmit *et al.*, 1986; de Waele *et al.*, 1986, 1988) and electron microscopy (EM; Faulk and Taylor, 1971; Walther and Muller, 1986; Baschong and Wrigley, 1990). To increase the visibility of these labels and the sensitivity of the method, the immunogold–silver staining technique (Danscher, 1981; Holgate *et al.*, 1983) is used.

One of the youngest microscopic techniques is the atomic force microscope (AFM; Binnig *et al.*, 1986) or scanning force microscope. This technique can yield high-resolution images of sample surfaces, even in an aqueous environment, and has therefore great potential for biological objects. Although many cell surface features, such as membrane-specific molecules or receptor sites can be assessed, the direct structural identification of specific structures on the surface of cells is currently not possible due to the limited resolution of the AFM on heterogeneous biological objects. The need for a specific labeling technique for the AFM has been recognized by us and other groups (Putman *et al.*, 1993a,c; Butt *et al.*, 1990; Hoh and Hansma, 1992). Recently we showed that *in situ* hybridization probes can be visualized in AFM by detection of the precipitated product of a peroxidase/diaminobenzidine reaction (Putman *et al.*, 1993c; Rasch *et al.*, 1993). Immunogold labels (antibody conjugated with colloidal gold) in combination with AFM have been reported by Häberle *et al.* (1991) and Putman *et al.* (1993a) for cell surface labeling, by Shaiu *et al.* (1993a,b) for detection of DNA, and by Mulhern *et al.* (1992) for studies of interaction of antibodies to biological surfaces.

In a previous paper we have shown that the round morphology of small gold particles linked to antibodies can be recognized in the AFM images of human lymphocytes (Putman *et al.*, 1993a) for gold particles with a diameter of 30 nm. It was also shown that increasing the size of the particles by deposition of a silver layer (silver enhancement) increased the visibility of the label. However, the number of gold particles on the cell surface was surprisingly low. Moreover, it was not always possible to discriminate between labels and globular protrusions of the cell membrane.

1047-8477/94 $6.00

In this paper we present a further study on human lymphocytes labeled with immunogold labels of 1 and 30 nm in size and different times of silver enhancement. Our first goal is to investigate the reliability of the AFM identification of antigens on cell membranes. Therefore, we made a direct comparison between AFM images and other more established techniques: bright-field and fluorescence microscopy and flow cytometry. We present images of the same double-labeled cells obtained by bright-field microscopy, fluorescence microscopy, and AFM. The results illustrate the potential of precise membrane protein localization with the AFM approach. Good correlation between force and optical microscopy indicates that the immunogold particles can be used as cell surface markers, with the advantage of at least one order of magnitude higher lateral resolution in AFM. The final goal will be the analysis of the cell surface structures at high resolution. The procedure should be as follows. First, the AFM imaging of the cell membrane before silver enhancement. Second, AFM imaging of the same cell after silver enhancement and finally the comparison of the surface structure as visualized in the two AFM images.

MATERIALS AND METHODS

Sample Preparation

Immunogold particles on glass. Microscope cover glasses were coated with poly-L-lysine by keeping them in a diluted solution of 0.01% poly-L-lysine in phosphate-buffered saline (PBS) overnight. Goat anti-mouse linked to colloidal gold particles 1 or 30 nm in size (GAM.IgG1, GAM.IgG30) Auroprobe LM (Janssen, Belgium) was diluted 1:20 with PBS (pH 7.3) and applied on a coated microscope cover glass for 1–3 hr. The samples were rinsed with PBS and MilliQ_{UF} water and air dried. Afterward the silver enhancement procedure using a commercially available kit (intenSE M-kit, Janssen Pharmaceutica, Beerse, Belgium) was performed according to the manufacturer's prescription, for different times, up to 40 min.

Preparation of lymphocytes. Human blood was obtained by venipuncture from a healthy individual, where heparin was used as anti-coagulant. Peripheral blood lymphocytes were obtained using the Percoll density separation method (density 1.077 g/cm^3). To eliminate monocytes, the cell suspension was incubated in a culture flask for 1 hr at 37°C in a 5% CO_2 incubator. The cell suspension was adjusted to a concentration of 10^6/ml in PBS containing 1% bovine serum albumin and 0.005% sodium azide. Then the cell suspension was incubated with 10 μl of monoclonal antibody anti-CD3–FITC (fluorescein isothiocyanate) (Becton–Dickinson, San Jose, CA) for 30 min, on ice in the dark. After washing two times, the cells were then incubated with 100 μl of 1:20 diluted secondary antibody goat anti-mouse (GAM.IgG1, GAM.IgG30) for 60 min at room temperature. After two washing steps cytospin slides were prepared for imaging with AFM and LM. These were then fixed in buffered paraformaldehyde acetone (pH 6.7; concentration 9.25%). Several fixation solutions (formaldehyde acetone, paraformaldehyde acetone, ethanol:glacial acetic acid 95:5) have been tried in order to have good results both in fluorescence emission of FITC and silver enhancement of gold particles. The best results were obtained with paraformaldehyde acetone. The silver enhancement procedure was performed as described above. For flow cytometry the cell suspensions were prepared as mentioned above, but after labeling with secondary antibodies GAM.IgG1 or GAM.IgG30, the cells were fixed with 1% paraformaldehyde.

Fluorescence Microscope

The cytospin preparations were examined by bright-field and fluorescence microscopy (Olympus inverted research microscope Model IMT-2). The microscope was equipped with an intensified CCD camera, a preprocessor, and PC-Argus software (Hamamatsu Photonics). Bright-field and fluorescence images of the cells were obtained using a 40× objective (D Plan Apo 40× uv; NA = 1.00; oil immersion) and a magnification changer 1.5×. FITC has the excitation band in blue (450–499 nm) and are emission spectrum in green/yellow (510–540 nm).

Atomic Force Microscope

The AFM used in this study is a home-built stand-alone AFM. The development of the compact stand-alone AFM is described in more detail elsewhere (Van der Werf *et al.*, 1993; Putman *et al.*, 1993b). This design permits imaging of samples of any kind and size because the tip and not the sample is scanned. More important with respect to biological applications is the fact that this AFM can be combined with an inverted optical microscope. While scanning, the surface features cause deflections of the cantilever. These cantilever displacements are detected with the optical beam deflection technique (Meyer and Amer, 1988; Putman *et al.*, 1992b). The data presented here were obtained using two modes of operation: the height mode and the error signal mode (Putman, 1992a). In the height mode, a feedback loop keeps the deflection of the cantilever (applied force) constant. The voltage applied to the z-electrode of the piezo is plotted as a function of the spatial position. In this mode of operation the height of the gold particles is measured correctly. In the error signal mode the residual variations in force which are not compensated by the feedback loop (due to the limited band width of the loop) are displayed. The feedback loop can be viewed as a high-pass filter: only topographic features with higher spatial frequencies cause cantilever deflections and are acquired. This mode is particularly useful in the detection of small labels on relatively large cell surfaces. Accurate height information, however, is not obtained in this mode. Since in the error signal mode the edges of surface features are enhanced due to the compensation by the feedback loop, bright shades correspond to the up slope and dark shades to the down slope of a feature. The images presented in this study are recorded in the error signal mode unless noted otherwise. Height information mentioned in the results were obtained from height images (not shown) recorded simultaneously with the error images. At cell edges one can observe tip artifacts due to the steep slope of the cells, demonstrating that in AFM the resulting images are influenced by both the tip shape and the morphology of the object. Images (300 × 300 datapoints) were obtained at a scan rate of 15 lines per second resulting in an imaging time of 20 sec per image. We used a 200-μm-long Si_3N_4 cantilever (with an integrated pyramidal tip; Digital Instruments, Santa Barbara, CA) with a spring constant of 0.12 N/m and the loading force was about 10^{-8} N.

Flow Cytometer

Experiments were performed with a home-built flow cytometer equipped with an argon-ion laser (Spectra-Physics) tuned to 488 nm. The instrument is comparable to commercially available instruments and has been described elsewhere (Terstappen *et al.*, 1986; Bakker Schut *et al.*, 1993). In brief, a vertically polarized laser beam is focused at cells passing one by one in a flow cell. Forward and orthogonal elastic scattering are acquired. In general, the forward scatter gives information on the size of the cells and the orthogonal scatter gives structural information of the cell, including the cell surface. In addition, fluorescence emitted

by dyes on labeled cells can be obtained. Thus, FITC fluorescence was measured using the green fluorescence channel (510–550 nm) and the (silver-enhanced) GAM.IgG1 or GAM.IgG30 labeled cells were detected by orthogonal light scattering. In a single run, 4096 cells are analyzed and this takes 1–5 sec.

RESULTS AND DISCUSSION

As stated in the Introduction, one of the major advantages of the AFM is that it can also be operated under physiological conditions. At the moment, however, it is still not a trivial matter to image cells in liquid. To limit the problems while developing the labeling methodology as presented here, we have chosen to do the labeling experiments on dried samples.

Colloidal gold particles of 1 and 30 nm in size, linked to antibodies, were deposited on a glass slide. The AFM was used to image these gold particles without and with silver enhancement with an increasing development time. From these images, the height of a large number of particles has been determined. The mean value of these particles was plotted as a function of time (Fig. 1). The deposition of silver during enhancement was not uniform (as is known from EM) showing a large variation in enhanced particles size as indicated by the error bars. There is no data point for the 1-nm gold particle without silver enhancement (time: 0 min) because the roughness of the glass is about 2 nm. Initial measurements on dried cells revealed a surface roughness of 20–30 nm. Therefore, it is not reliable to use 1 and 30 nm gold particles without silver enhancement.

A system combining a stand-alone AFM and an inverted fluorescence microscope was used to obtain images of the same cells. Figure 2 shows the images of lymphocytes labeled with CD3.FITC + GAM.IgG30 and silver enhanced for 30 min. Figures 2A and 2B show images of labeled cells obtained with the LM (bright-field and fluorescence). The size of a lymphocyte is typically 15 μm. In the bright-field image (Fig. 2A) no clear distinction could be made between CD3-positive cells and CD3-negative cells. The bright fluorescent cells (Fig. 2B) are CD3-positive T-lymphocytes. Figure 2C presents the AFM image of the same group of cells and Figs. 2D and 2E show details of the surfaces of a CD3-positive cell (bright fluorescence) and a CD3-negative cell (low fluorescence) at a higher magnification. It is clear that the CD3-negative cells exhibit a low number of particles, whereas CD3-positive cells exhibit many particles. The height of the enhanced gold particles on the cell surface (about 100 nm) is somewhat smaller than the height of the particles measured on a flat glass surface after the same enhancement time (about 140 nm; see Fig. 1). This may indicate that the particles are partly embedded in the cell membrane.

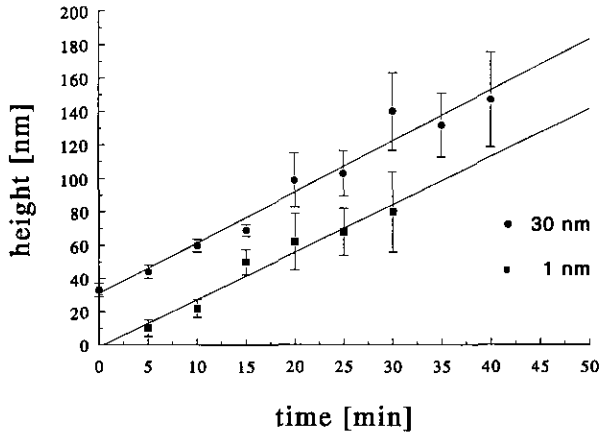

FIG. 1. Time dependence of the height of gold particles 1 and 30 nm on glass, during the silver-enhancement process as measured with the AFM.

In Fig. 3 we show lymphocytes labeled with 1-nm gold particles after 30 min silver enhancement. Figures 3A and 3B show the bright-field and fluorescence images, respectively (same magnification). After silver enhancement the CD3-positive cells (bright fluorescence) in bright-field images revealed dark granules on their surface membranes, which may represent clusters of particles. Thus, a positive cell is bright in the fluorescence image, but shows up as a dark cell in the bright-field (absorption) image. Figure 3C shows the AFM image of the same group of cells and Figs. 3D and 3E show a magnification of the surface of a positive and a negative cell, respectively. The images clearly demonstrate the good correlation between the atomic force microscopic images and the optical images. Artifacts due to tip-object convolution are evident at the cell edges (see Fig. 3D). Figure 3F shows the AFM image of a cell which is only CD3-positive on the right side (as can be seen in both bright-field and fluorescence images). This is probably due to capping induced by antibodies.

Lymphocytes labeled with 1-nm gold particles and 15-min silver enhancement are presented in Fig. 4. The height of the enhanced particles is in the range of roughness of the surface (20–30 nm); therefore, the particles (Fig. 4E) can hardly be discriminated from the surrounding membrane: sphere-like structures on the surface cannot be distinguished from the probe. It is obvious that the facility of imaging small particles with AFM depends on the roughness of the cell surface.

We have observed that red blood cells have a lower surface corrugation than white blood cells; thus, it should be more easy to visualize small-size particles on the cell surface of red blood cells. In Fig. 5 the AFM image of a red blood cell is shown. The transferrin receptor of the red blood cell is detected

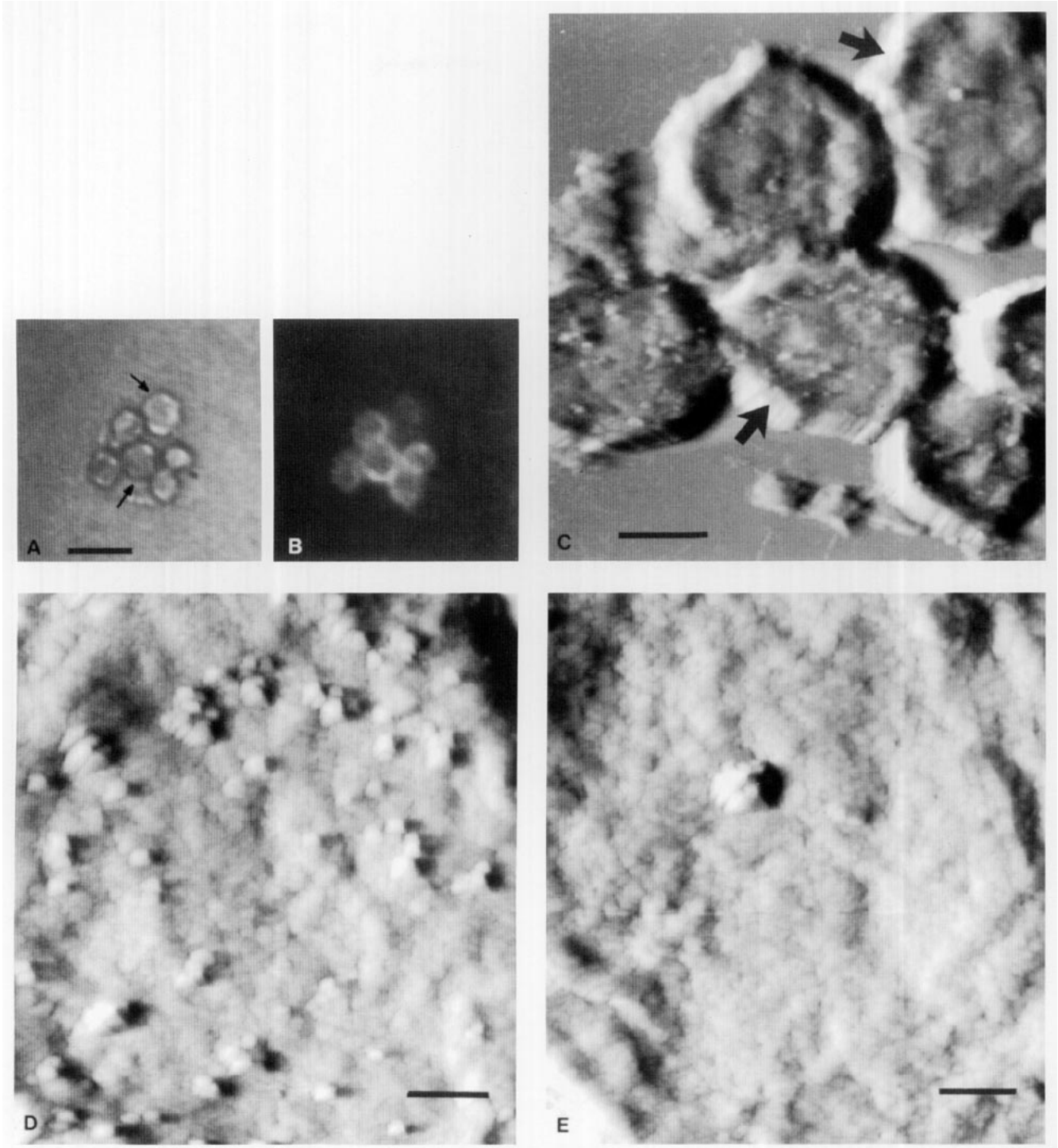

FIG. 2. Group of air-dried lymphocytes double-labeled with immunogold (30 nm) and FITC after 30 min silver enhancement. The cells selected for AFM imaging are indicated by arrows. (A) Bright-field and (B) fluorescence image both at the same magnification; bar, 20 μm. (C) AFM image of the same group of cells; bar, 5 μm. (D) AFM image of a CD3-positive T-lymphocyte, identified on the basis of FITC fluorescence; bar, 1 μm. (E) AFM image of a CD3-negative lymphocyte, identified on the basis of FITC fluorescence; bar, 1 μm. AFM images are recorded in the error signal mode.

using superparamagnetic beads (5 nm) coupled to antibodies. These superparamagnetic beads are normally used for cell separation purposes. Almost the whole cell imaged with the AFM can be seen in Fig. 5A. The size of the red blood cell is about 10 μm. This is somewhat larger than the normal 7 to 8 μm and is caused by the cytospin preparation (at 500g) of the sample. Also the typical doughnut shape has

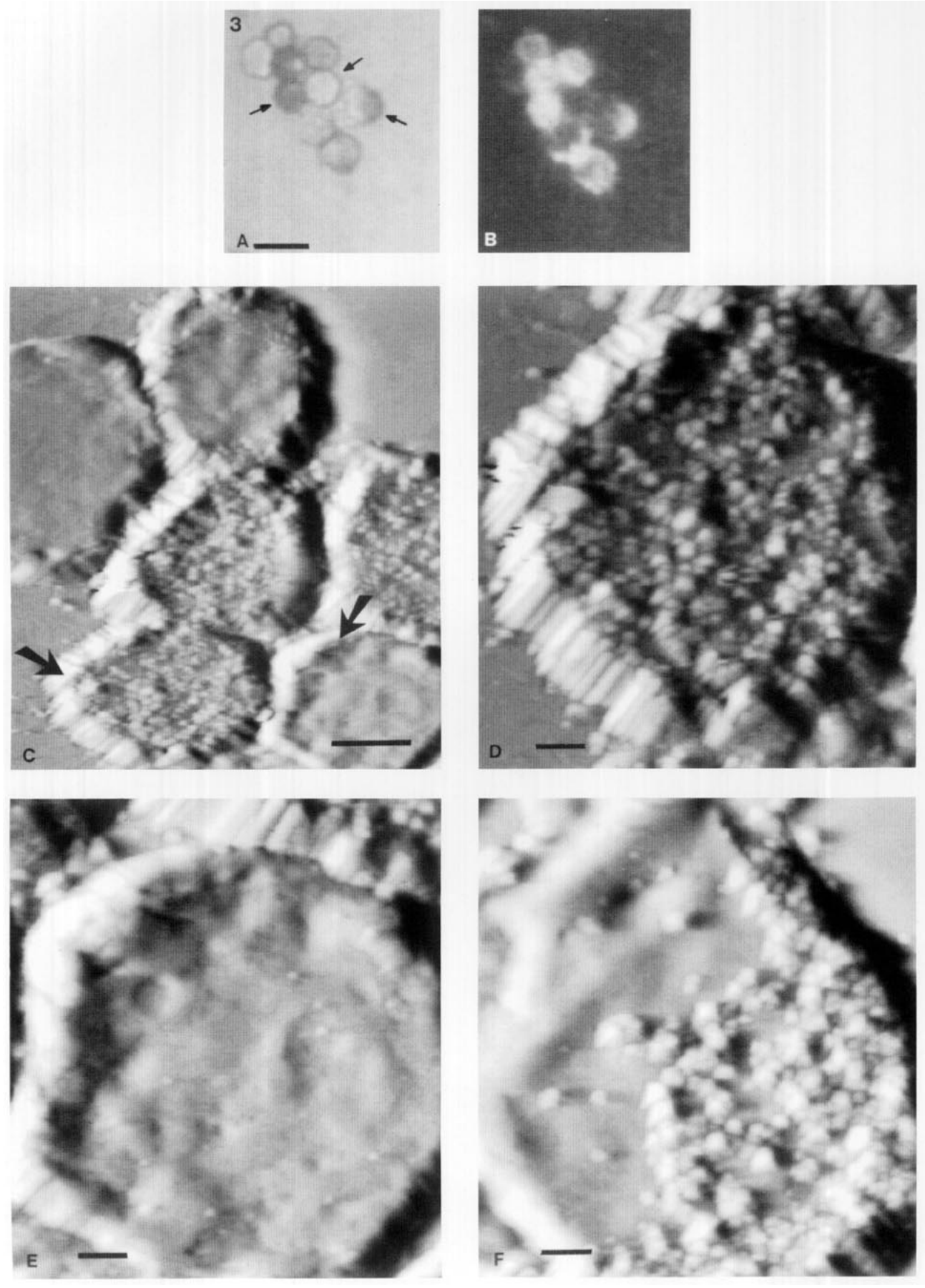
3
A
B
C
D
E
F

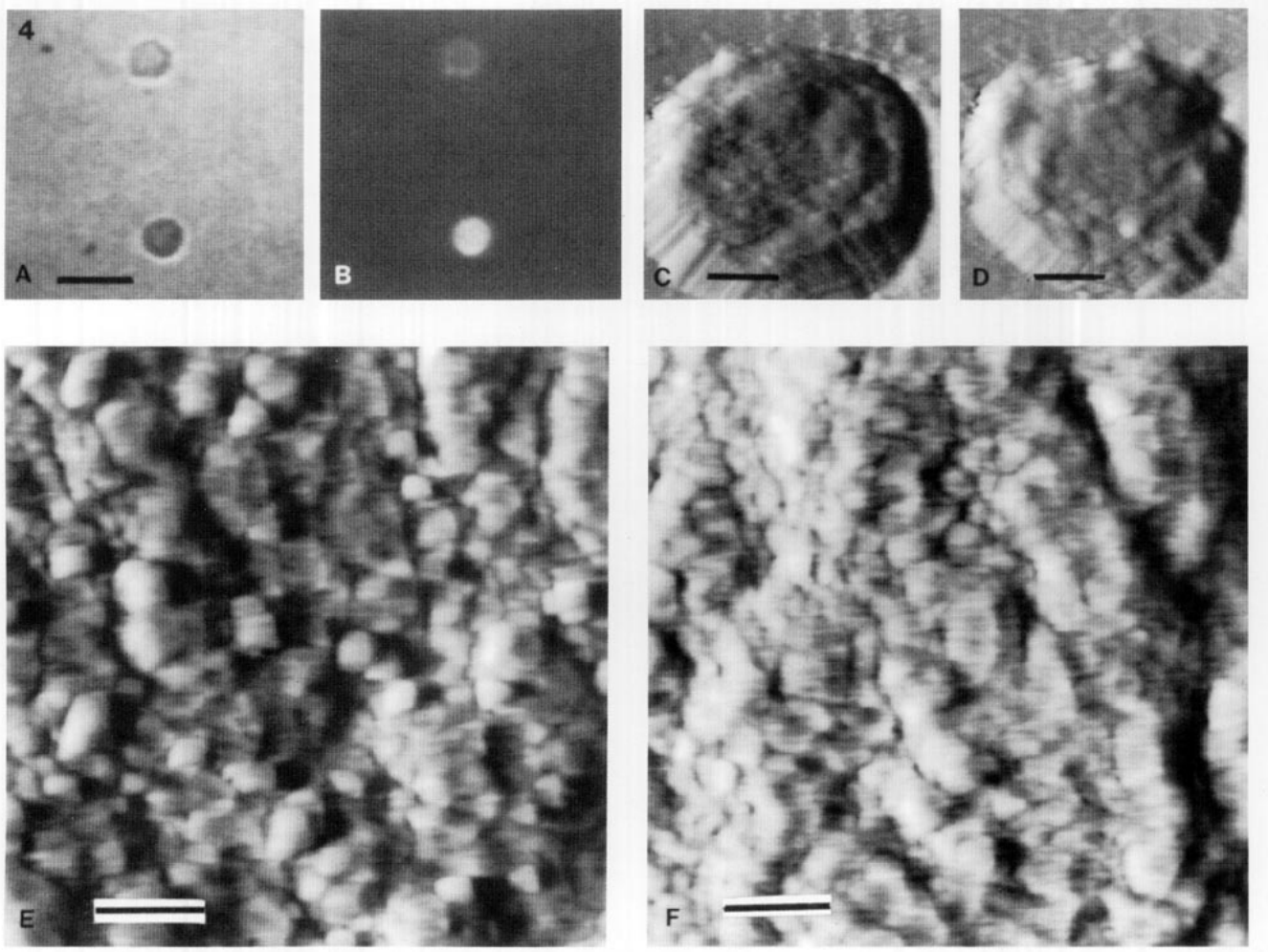

FIG. 3. Air-dried lymphocytes double-labeled with immunogold (1 nm) and FITC after 30 min silver enhancement. The cells selected for AFM imaging are indicated by arrows. (A) Bright-field and (B) fluorescence image both at the same magnification; bar, 20 μm. (C) AFM image of the upper part of the group of cells; bar, 5 μm. (D) AFM image of a CD3-positive T-lymphocyte, identified on the basis of FITC fluorescence; bar, 1 μm. (E) AFM image of a CD3-negative lymphocyte, identified on the basis of FITC fluorescence; bar, 1 μm. (F) AFM image of a lymphocyte which is CD3-positive only on the right side, which may be due to capping of the antigens induced by antibodies; bar, 1 μm. AFM images are recorded in the error signal mode.

FIG. 4. Air-dried lymphocytes double-labeled with immunogold (1 nm) and FITC after 15 min silver enhancement. (A) Bright-field and (B) fluorescence image both at the same magnification; bar, 20 μm. (C) AFM image of a CD3-positive T-lymphocyte, identified on the basis of FITC fluorescence (cell at the bottom in (B); bar, 2 μm. (D) AFM image of the CD3-negative lymphocyte (cell at the top in (A) and (B); bar, 2 μm. (E) AFM image of a detail of the CD3-positive cell in (C); bar, 0.5 μm. (F) AFM image of a detail of the CD3-negative cell in (D); bar, 0.5 μm. AFM images are recorded in error signal mode.

disappeared (partly caused by the error signal mode) and a large spread in cell diameters, ranging from 7 to 11 μm, has been observed by the optical microscope. AFM images of the cell surface at higher magnification are shown in Figs. 5B and 5C. The measured heights of the beads are between 5 and 8 nm with lateral dimensions of 20 to 30 nm caused by tip-object convolution. The roughness of the cell surface is 1.5 to 2.5 nm. Thus, for a smooth cell surface smaller particles can be used.

From Figs. 2, 3, and 4 it is clear that the smallest gold particles give a denser labeling than larger particles, indicating that more antigen sites are localized. This is probably due to a reduced steric hindrance, which inhibits the bonding between the conjugated antibody (coupled to the colloidal gold) and the antigen on the cell surface, giving smaller particles a higher labeling efficiency. Furthermore, AFM images of cells labeled with 1-nm gold show a more uniform distribution of particles on the membrane, when compared to cells labeled with 30 nm. This was confirmed by bright-field images where 1-nm labeled cells appear much darker than 30-nm labeled cells (Figs. 2A vs 3A). The same holds for the fluorescence images: 1-nm labeled cells appear much brighter than the 30-nm labeled cells (Figs. 3B vs. 2B).

Flow cytometry is another technique which makes

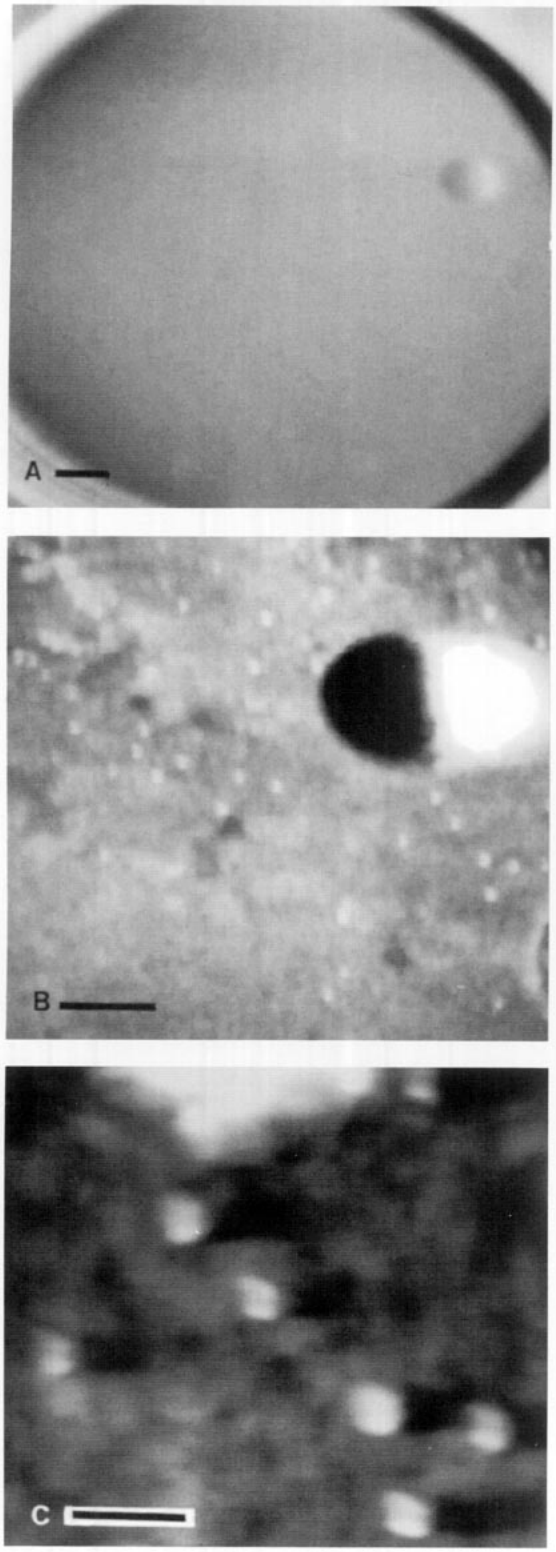

FIG. 5. AFM images of an air-dried red blood cell (erythrocyte). The labels are 5-nm superparamagnetic beads coupled to antibody against transferrin receptors (A) bar, 1 μm. (B) Detail of the surface; bar, 0.5 μm. (C) higher magnification; bar, 0.1 μm. (A,B) Error signal mode, (C) height mode and the grey levels from dark to bright correspond to about 10 nm.

possible a rapid verification of the correlation between the fluorescent and the immunogold silver-enhancement labeling procedures on a large number of cells (thousands). Böhmer and King (1984) showed that lymphocytes labeled with 40-nm gold particles (without silver enhancement) as secondary labels can be discriminated from unstained lymphocytes by flow cytometry, due to increased orthogonal light scatter. To increase the light scatter signal of the immunogold particles (1 and 30 nm) we used the silver-enhancement procedure (Garritsen, 1993) analogous to the procedure of de Waele *et al.* (1986) used in light microscopy. With 1- and 30-nm colloidal gold labeled lymphocytes without silver enhancement no differences in light scattering properties between positive and negative cells could be observed (Figs. 6A and 6C); in both scatter plots "forward vs orthogonal" only one cluster is present. After silver enhancement differences in scattering parameters are evident (Figs. 6C and 6D), especially in the case of the 1-nm gold particles. Positive cells (high FITC fluorescence) display a distinctive increase in orthogonal light scattering, whereas negative cells (low FITC fluorescence) show the same orthogonal light scatter as in the case of no silver enhancement (compare "FITC vs orthogonal" in the various situations). Using colloidal gold of different sizes, 1 nm (Figs. 6C and 6D), 30 nm (Figs. 6A and 6B), similar trends were observed but the separation between the clusters of positive and negative cells is more distinct for 1 than for 30 nm. This again indicates that more binding sites are localized by the smaller labels than by the larger labels, due to a lower steric hindrance for the small labels. The good agreement between FITC-labeled cells and the cells with an increased orthogonal light scattering for 1-nm gold spheres is in agreement with the observations by AFM and fluorescence microscopy. A phenomenon which is also observed from flow cytometer data is an increase of the FITC fluorescence before (Figs. 6A and 6C) and after silver enhancement (Figs. 6B and 6D). This could be due to differences in pH or the media used, but understanding of this effect requires further studies.

As stated above the microscopical experiments have been performed on air-dried cells for the sake of simplicity. We see, however, no reason why the results obtained will not be valid for living cells also.

CONCLUSIONS

A system combining a stand-alone AFM and an inverted fluorescence microscope was used to obtain force and fluorescence images of the same double-labeled cell. It was shown that particles after silver enhancement which are detected on the cell surface of human lymphocytes with AFM are only detected on cells that are marked as positive on the basis of

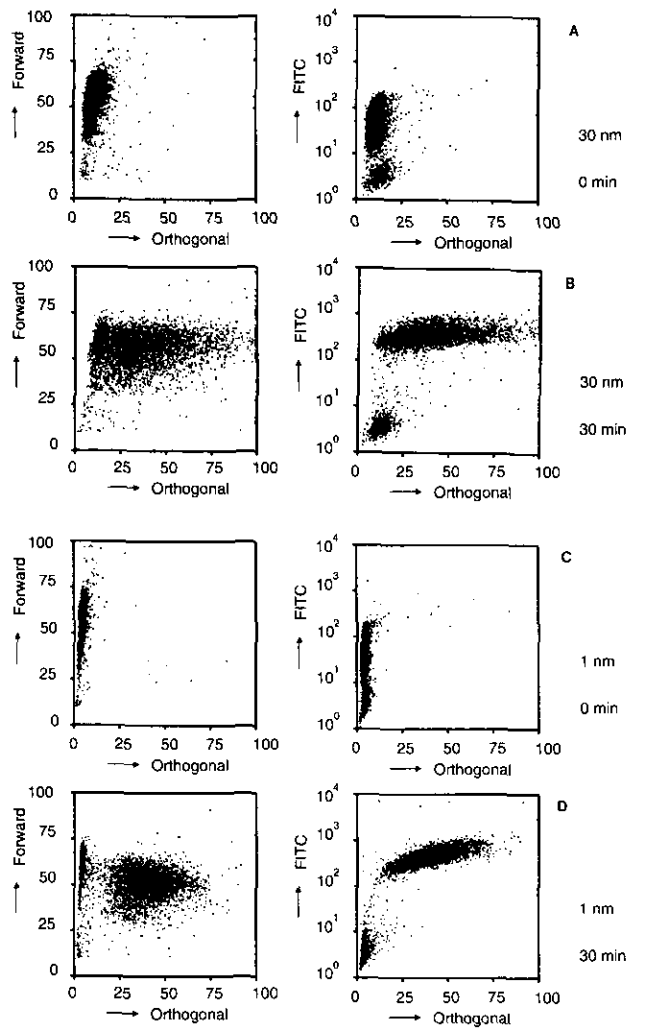

FIG. 6. Flow cytometer data of lymphocytes double-labeled with immunogold (1 or 30 nm) and FITC show the increase in orthogonal light scattering for CD3-positive T-lymphocytes after silver enhancement. (A) Lymphocytes, double-labeled with immunogold (30 nm) and FITC, without silver enhancement. (B) Lymphocytes as in (A), but after 30 min silver enhancement. (C) Lymphocytes double-labeled with immunogold (1 nm) and FITC, without silver enhancement. (D) Lymphocytes as in (C), but after 30 min silver enhancement.

immunofluorescence. Immunogold labels of 1 nm gave better results than 30-nm immunogold labels in terms of specificity and number of detected particles. A combination of small immunogold labels gold (1 nm) and silver enhancement is the best option for the detection of specific membrane proteins and structural studies of the cell membrane with the AFM. The results using different techniques are in good agreement.

We thank Ine Segers for the preparation of the samples and Dr. Henk Garritsen for sample of red blood cells with magnetic beads. This research was supported by the Dutch Organization for Scientific Research (NWO). C.R.N. was supported via a TEMPUS program of the European Community.

REFERENCES

Bakker Schut, T. C., Florians, A., van der Werf, K. O., and de Grooth, B. G. (1993) Flow cytometry data processing and data acquisition with a personal computer using an RTI-800 multifunction A/D I/O board, *Rev. Sci. Instrum.* **64**, 3116.

Baschong, W., and Wrigley, N. G. (1990) Small colloidal gold conjugated to Fab fragments or immunoglobulin G as high-resolution labels for electron microscopy: A technical overview, *J. Electron Microsc. Tech.* **14**, 313.

Binnig, G., Quate C. F., and Gerber, Ch. (1986) Atomic force microscopy, *Phys. Rev. Lett.* **56**, 930.

Böhmer, R. M., and King, N. J. C. (1984) Flow cytometric analysis of immunogold cell surface label, *Cytometry* **5**, 543.

Butt, H. J., Wolff, E. K., Gould, S. A. C., Dixon Northern, B., Peterson, C. M., and Hansma, P. K. (1990) Imaging cells with the atomic force microscope, *J. Struct. Biol.* **105**, 54.

Danscher, G. (1981) The localization of gold in biological tissue: A photochemical method for light and electron microscopy, *Histochemistry* **71**, 81.

de Waele, M., De Mey, J., Renmans, W., Labeur, C., Reynaert, Ph., and van Camp, B. (1986) An immunogold-silver staining method for detection of cell-surface antigens in light microscopy, *J. Histochem. Cytochem.* **34**, 935.

de Waele, M., Renmans, W., Segers, E., Jochmans, K., and van Camp, B. (1988) Sensitive detection of immunogold-silver staining with dark field and epipolarization microscopy, *J. Histochem. Cytochem.* **36**, 679.

Faulk, W. P., and Tayler, G. M. (1971) An immunocolloid method for the electron microscopy, *Immunocytochemistry* **8**, 1081.

Garritsen, H. S. P. (1993) Immunophenotypic and Functional Studies of Lymphocytes from Patients with Acute Myeloid Leukaemia, Ph.D. thesis, University of Twente, The Netherlands.

Häberle, W., Hörber, J. K. H., and Binnig, G. (1991) Force microscopy on living cells, *J. Vac. Sci. Technol.* **B9**, 121.

Hoefsmit, E. C. M., Korn, C., Blijleven, N., and Ploem, J. S. (1986) Light microscopical detection of single 5 and 20 nm gold particles used for immunolabeling of plasma membrane antigens with silver enhancement and reflection contrast, *J. Microsc.* **143**, 161.

Hoh, J. H., and Hansma, P. K. (1992) Atomic force microscopy for high-resolution imaging in cell biology, *Trends Cell Biol.* **2**, 208.

Holgate, C. S., Jackson, P., Cowen, Ph. N., and Bird, C. C. (1983) Immunogold–silver staining: New method of immunostaining with enhanced sensitivity, *J. Histochem. Cytochem.* **31**, 938.

Meyer, G., and Amer, N. M. (1988) Novel optical approach to atomic force microscopy, *Appl. Phys. Lett.* **53**, 2400.

Mulhern, P. J., Blackford, B. L., Jericho, M. H., Southam, G., and Beveridge, T. J. (1992) AFM and STM studies of the interaction of antibodies with S-layer sheath of the archaeobacterium *Methanospirillum hungatei*, *Ultramicroscopy* **42–44**, 1214.

Putman, C. A. J., van der Werf, K. O., de Grooth, B. G., Greve, J., van Hulst, N. F., and Hansma, P. K. (1992a) New imaging mode in atomic force microscopy based on the error signal, *Proc. SPIE* **1936**, 198.

Putman, C. A. J., de Grooth, B. G., van Hulst, N. F., and Greve, J. (1992b) A detailed analysis of the optical beam deflection technique for use in atomic force microscopy, *J. Appl. Phys.* **72**, 6.

Putman, C. A. J., de Grooth, B. G., Hansma, P. K., van Hulst, N. F., and Greve, J. (1993a) Immunogold labels: Cell-surface markers in atomic force microscopy, *Ultramicroscopy* **48**, 177.

Putman, C. A. J., van Leeuwen, A. M., de Grooth, B. G., Radosevic, K., van der Werf, K. O., van Hulst, N. F., and Greve, J.

(1993b) Atomic force microscopy combined with confocal laser scanning microscopy: A new look at cells, *Bioimaging* 1, 63.

Putman, C. A. J., de Grooth, B. G., Wiegant, J., Raap, A. K., van der Werf, K. O., van Hulst, N. F., and Greve, J. (1993c) Detection of in situ hybridization to human chromosomes with the atomic force microscope, *Cytometry* 14, 356.

Rasch, P., Wiedemann, U., Wienberg, J., and Heckl, W. M. (1993) Analysis of banded human chromosomes and in situ hybridization patterns by scanning force microscopy, *Proc. Natl. Acad. Sci. USA* 90, 2509.

Shaiu, W.-L., Vesenka, J., Jondle, D., Henderson, E., and Larson, D. D. (1993a) Visualization of circular DNA molecules labeled with colloidal gold spheres using atomic force microscopy, *J. Vac. Sci. Technol.* A11, 820.

Shaiu, W.-L., Larson, D. D., Vesenka, J., and Henderson, E. (1993b) Atomic force microscopy of oriented linear DNA molecules labeled with 5 nm gold spheres, *Nucleic Acids Res.* 21, 99.

Terstappen, L. W. M. M., de Grooth, B. G., Nolten, G. M. J., ten Napel, C. H. H., van Berkel, W., and Greve, J. (1986) Physical discrimination between human T-lymphocyte subpopulation of T8-positive cells, *Cytometry* 7, 178.

Van der Werf, K. O., Putman, C. A. J., de Grooth, B. G., Segerink, F. B., Schipper, E. H., van Hulst, N. F., and Greve, J. (1993) Compact stand-alone atomic force microscope, *Rev. Sci. Instrum.* 64, 2892.

Walther, P., and Muller, M. (1986) Detection of small (5–15 nm) gold labeled surface antigens using backscattered electrons, *in* Muller, M., Becker, R. P., Boyde, A., and Wolosewick, J. J. (Eds.), p. 195, Science of Biological Specimen Preparation, SEM, Chicago.